Supplementary Information

High Performance Complementary WS_2 Devices with Hybrid Gr/Ni Contacts

Muhammad Farooq Khan[1†*], Faisal Ahmed[2,3†], Shania Rehman[1], Imtisal Akhtar[4], Malik Abdul Rehman[5], Pragati A. Shinde[5], Karim Khan[6,7], Deok-kee Kim[1], Jonghwa Eom[8], Harri Lipsanen[2] and Zhipei Sun[2]

[1]Department of Electrical Engineering, Sejong University, 209 Neungdong-ro, Gwangjin-gu, Korea. [2]Department of Electronics and Nanoengineering, Aalto University, P.O. Box 13500, FI-00076 Aalto, Finland. [3]Department of Mechanical Engineering, College of Electrical and Mechanical Engineering, National University of Science and Technology, Islamabad 44000, Pakistan. [4]Department of Mechanical Engineering, Chung-Ang University, Seoul, South Korea. [5]School of Mechanical Engineering, Yonsei University, 50 Yonsei-ro, Seodaemun-gu, Seoul 03722, South Korea. [6]School of Electrical Engineering & Intelligentization, Dongguan University of Technology (DGUT), Dongguan, 523808, Guangdong, China. [7]Institute of Microscale Optoelectronics, Collaborative Innovation Centre for Optoelectronic Science & Technology, Key Laboratory of Optoelectronic Devices and Systems of Ministry of Education and Guangdong Province, College of Physics and Optoelectronic Engineering, Shenzhen Key Laboratory of Micro-Nano Photonic Information Technology, Guangdong Laboratory of Artificial Intelligence and Digital Economy (SZ), Shenzhen University, Shenzhen 518060, P.R. China. [8]Graphene Research Institute-Texas Photonics Center International Research Center (GRI-TPCIRC), Sejong University, Seoul 05006, Korea.

†These authors contributed equally to this work

***Corresponding email:** mfk@sejong.ac.kr

1. **Thickness of WS_2 flake**
2. **8 nm thick WS_2 device results**
3. **Arrhenius plots of Ni and Gr/Ni contacted WS_2 device**
4. **Extraction of Contact Resistance**
5. **Comparative Table of WS_2 and MoS_2 based *p-n* junctions**
6. **Comparative table of photoresponsivity of WS_2 and MoS_2 based devices**

1. Thickness of WS_2

Atomic force microscopy was employed to ascertain the thickness of WS_2 flakes. For given device, the topographic image of WS_2 flake was collected by scanning AFM in the square region of Figure S1(a) is shown in Figure S1(b). The height profile of the WS_2 flake is collected along the indicated path. Figure S1(c) represents that the WS_2 flake is ~14 nm thick.

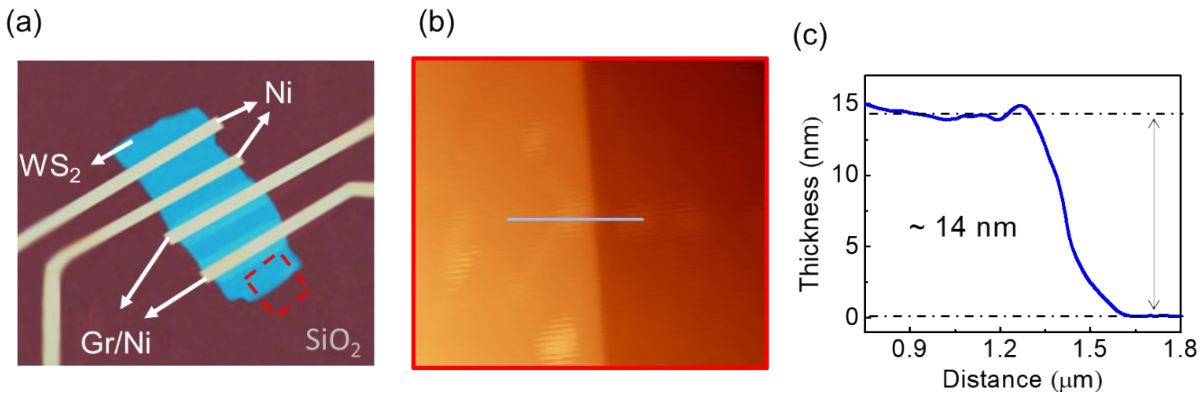

Figure S1. Thickness of WS_2 flake: (a) is the OM image of the WS_2 back gate devices with the Ni and the hybrid Gr/Ni contacts. **(b)** AFM topographic image of the WS_2 flake as indicated by red box in (a). The blue line is the scanning path to obtain the thickness profile. **(c)** The obtained thickness profile WS_2 flake collected from the AFM image.

2. 8 nm thick WS_2 device data

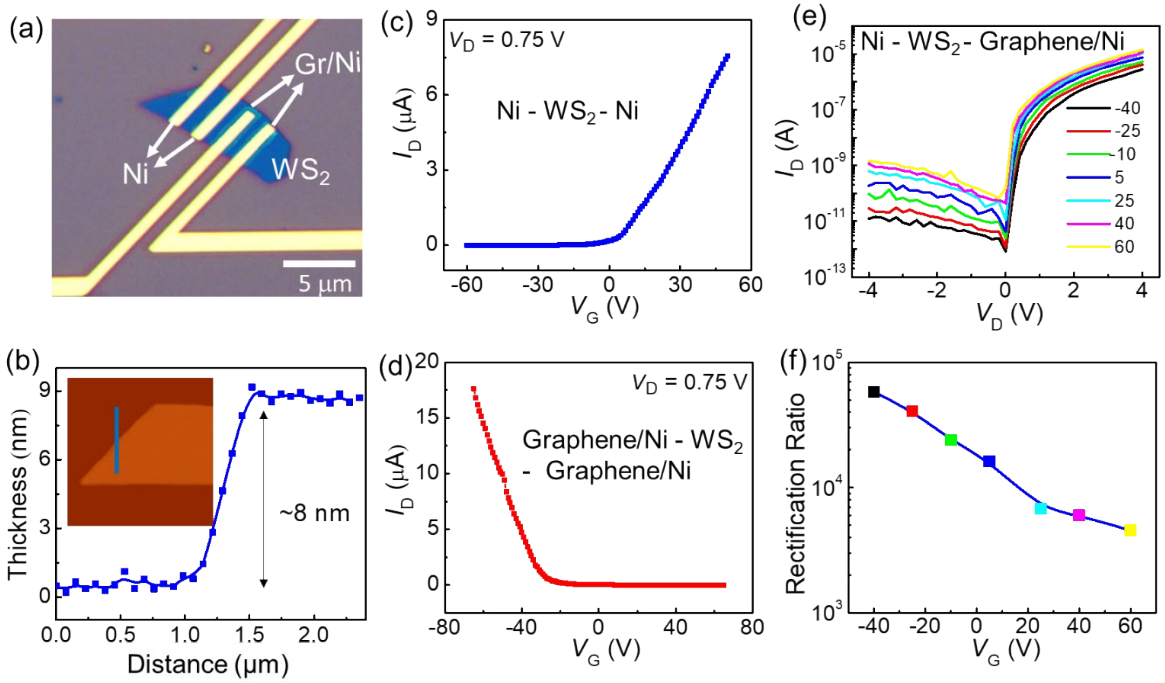

Figure S2. 8 nm thick WS_2 device: (a) is the optical micrograph image of the 8 nm thick WS_2 devices with the Ni/Au and the hybrid Gr/Ni contacts. **(b)** The thickness profile of WS_2 flake obtained along the blue line shown in AFM image in inset. **(c)** & **(d)** are the transfer curves of the Ni-contacted WS_2 device and the Gr/Ni contacted WS_2 device at V_D = 750 meV. **(e)** The output curves of asymmetrically contacted WS_2 device. **(f)** The rectification ratio (ratio of forward bias current to reverse bias current) as a function of gate bias, measured from plots shown in (e) at V_D = ± 2 V. Note that at same measurement conditions, the 8 nm thick WS_2 device shows higher rectification ratio as compared to 14 nm thick WS_2 device.

3. Arrhenius plots of Ni and Gr/Ni contacted WS_2 device

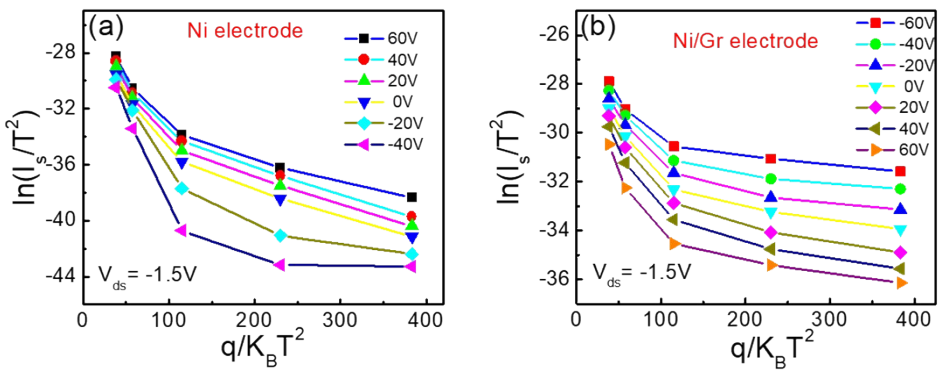

Figure S3. Arrhenius plots. The Arrhenius plots are extracted from the low temperature measurements at given back gate bias conditions. (a) for Ni contacted WS_2 device and (b) for Gr/Ni hybrid electrodes contacted WS_2 device. The decreasing slope of these curves gives the Schottky barrier height value for the corresponding interfaces, according to the equation (4) in main manuscript.

4. Extraction of Contact Resistance

Besides Schottky barrier height, contact resistance is another critical parameter to characterize the metal-semiconductor interface, and typically extracted by four-probe measurements or transfer length method. Given the two-probe geometry of our device, it is challenging to extract the contact R_c. However, the total device resistance in a device is comprised of channel resistance (R_{CH}) and twice of contact resistance (R_c). At large applied V_G, the carrier concentration in a device is increased. In result, the channel become highly conductive. In other words, R_{CH} becomes negligible, and the total device resistance approaches to the twice of R_C.[1] Using this scheme, we plotted the R_c for Ni-WS_2 and Gr/Ni-WS_2 interfaces from their respective transfer curves, as shown in Fig. S2. We understand that the measured R_c values are overestimated, and approaches to true value of R_C, as absolute value of V_G increases. Nonetheless, the V_G

dependent plots follow the typical *n*-type and *p*-type trends for Ni-contacted and Gr/Ni contacted WS_2 device.

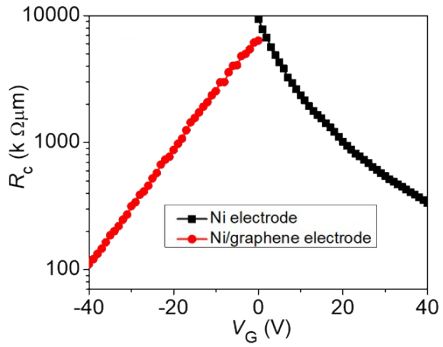

Figure S4: Contact resistance. The contact resistance as a function of V_G for Ni-contacted and Gr/Ni contacted WS_2 device.

5. Comparative Table of WS_2 and MoS_2 based *pn* junctions

S. No	Materials	Device Structure	Thickness (nm)	Rectification ratio	Ideality Factor	Voc (V)	Ref
1	WS_2	Hybrid contacts to WS_2	14	10000	1.6	0.31	This work
2	BP / WS_2	Planar heterostructure	7.6 / 9.5	26000	1.7	0.35	2
3	WS_2 / MoS_2	CVD grown Planar & Vertical Heterostructures	Monolayer/ Monolayer	100	NA	0.12	3
4	WS_2 / MoS_2	Vertical Heterostructure	Multilayer/ Multilayer	10000	NA	0.25	4
5	WSe_2 / WS_2	CVD grown Planar heterojunction	Multilayer	NA	NA	0.47	5
6	WS_2 / $ReSe_2$	Planar heterostructure	80 / 147	30	NA	NA	6
7	SnS / WS_2	CVD grown Vertical Heterostructure	200 / 0.7	15	3.8	NA	7
8	Gr/WS_2/Gr	Vertical FET	3.5	1000000	NA	NA	8
9	WS_2 / GaN	CVD grown WS_2 Heterojunction (2D-3D)	400	> 100	NA	NA	9
10	WS_2 / Si	Vertical heterostructure	54 / bulk	1000	NA	NA	10
11	MoS_2	Vertical & Chemical doping	3	100	1.6	0.6	11
12	MoS_2	Lateral Chemical doping	60	30	1	0.5	12
13	MoS_2	Thickness offset	6.9 / 0.65	1000	1.95	NA	13

6. Comparative table of photoresponsivity of WS_2 and MoS_2 based devices

S. No	Materials	Wavelength (nm)	Optical Power ($mWcm^{-2}$)	Responsivity (A/W)	Ref
1	14 nm WS_2-hybrid contacts	532	0.14	4×10^4	This work
2	14 nm WS_2-hybrid contacts	850	0.14	2×10^4	This work
3	6 nm WS_2	458	2*	2.1×10^{-5}	14
4	42 nm WS_2	633	30	5.7	15
5	20 nm WS_2	630	250	0.27	16
6	Gr/WS_2/Gr (5~50-layer WS_2)	633	10^{-6}*	0.1	17
7	Lateral WS_2/MoS_2	633	141	1.42	4
8	BP/WS_2	600	1.2×10^{-6}*	0.5	2
9	2L WS_2/graphene	532	2.7×10^5	0.74	18
10	0.65 nm MoS_2	561	2.38×10^5	880	19
11	0.65 nm MoS_2	532	8×10^4	7.5×10^3	20
12	2 nm MoS_2	532	2×10^3	5.7×10^{-1}	21
13	MoS_2 Chemical doping	500	-	5.07	12
14	15-19 nmMoS_2 pn junction	660	80	0.25	22
15	4 nm/28 nm $MoSe_2$ homojunction	635	14.4	550	23

**units in Watt*

Reference:

S1 N. Petrone, T. Chari, I. Meric, L. Wang, K. L. Shepard, J. Hone, T. Roy, M. Tosun, J. S. Kang, A. B. Sachid, S. B. Desai, M. Hettick, C. C. Hu and A. Javey, *ACS Nano*, 2014, **8**, 6259–6264.

S2 G. Dastgeer, M. F. Khan, G. Nazir, A. M. Afzal, S. Aftab, B. A. Naqvi, J. Cha, K.-A. Min, Y. Jamil, J. Jung, S. Hong and J. Eom, *ACS Appl. Mater. Interfaces*, 2018, **10**, 13150–13157.

S3 Y. Gong, J. Lin, X. Wang, G. Shi, S. Lei, Z. Lin, X. Zou, G. Ye, R. Vajtai, B. I. Yakobson, H. Terrones, M. Terrones, B. K. Tay, J. Lou, S. T. Pantelides, Z. Liu, W. Zhou and P. M. Ajayan, *Nat. Mater.*, 2014, **13**, 1135–1142.

S4 N. Huo, J. Kang, Z. Wei, S.-S. Li, J. Li and S.-H. Wei, *Adv. Funct. Mater.*, 2014, **24**, 7025–7031.

S5 X. Duan, C. Wang, J. C. Shaw, R. Cheng, Y. Chen, H. Li, X. Wu, Y. Tang, Q. Zhang, A. Pan, J. Jiang, R. Yu, Y. Huang and X. Duan, *Nat. Nanotechnol.*, 2014, **9**, 1024–1030.

S6 C. Wang, S. Yang, W. Xiong, C. Xia, H. Cai, B. Chen, X. Wang, X. Zhang, Z. Wei, S. Tongay, J. Li and Q. Liu, *Phys. Chem. Chem. Phys.*, 2016, **18**, 27750–27753.

S7 A. Sukma Aji, M. Izumoto, K. Suenaga, K. Yamamoto, H. Nakashima and H. Ago, *Phys. Chem. Chem. Phys.*, 2018, **20**, 889–897.

S8 T. Georgiou, R. Jalil, B. D. Belle, L. Britnell, R. V. Gorbachev, S. V. Morozov, Y.-J. Kim,

A. Gholinia, S. J. Haigh, O. Makarovsky, L. Eaves, L. A. Ponomarenko, A. K. Geim, K. S. Novoselov and A. Mishchenko, *Nat. Nanotechnol.*, 2013, **8**, 100–103.

S9 Y. Yu, P. W. K. Fong, S. Wang and C. Surya, *Sci. Rep.*, 2016, **6**, 37833.

S10 S. Aftab, M. F. Khan, K.-A. Min, G. Nazir, A. M. Afzal, G. Dastgeer, I. Akhtar, Y. Seo, S. Hong and J. Eom, *Nanotechnology*, 2018, **29**, 045201.

S11 H.-M. Li, D. Lee, D. Qu, X. Liu, J. Ryu, A. Seabaugh and W. J. Yoo, *Nat. Commun.*, 2015, **6**, 6564.

S12 M. S. Choi, D. Qu, D. Lee, X. Liu, K. Watanabe, T. Taniguchi and W. J. Yoo, *ACS Nano*, 2014, **8**, 9332–9340.

S13 M. Sun, D. Xie, Y. Sun, W. Li, C. Teng and J. Xu, *Sci. Rep.*, 2017, **7**, 4505.

S14 N. Perea-López, A. L. Elías, A. Berkdemir, A. Castro-Beltran, H. R. Gutiérrez, S. Feng, R. Lv, T. Hayashi, F. López-Urías, S. Ghosh, B. Muchharla, S. Talapatra, H. Terrones and M. Terrones, *Adv. Funct. Mater.*, 2013, **23**, 5511–5517.

S15 N. Huo, S. Yang, Z. Wei, S.-S. Li, J.-B. Xia and J. Li, *Sci. Rep.*, 2015, **4**, 5209.

S16 S. Hwan Lee, D. Lee, W. Sik Hwang, E. Hwang, D. Jena and W. Jong Yoo, *Appl. Phys. Lett.*, 2014, **104**, 193113.

S17 L. Britnell, R. M. Ribeiro, A. Eckmann, R. Jalil, B. D. Belle, A. Mishchenko, Y. J. Kim, R. V. Gorbachev, T. Georgiou, S. V. Morozov, A. N. Grigorenko, A. K. Geim, C. Casiraghi, A. H. C. Neto and K. S. Novoselov, *Science (80-.).*, 2013, **340**, 1311–1314.

S18 H. Huang, Y. Sheng, Y. Zhou, Q. Zhang, L. Hou, T. Chen, R.-J. Chang and J. H. Warner, *ACS Appl. Nano Mater.*, 2018, **1**, 6874–6881.

S19 O. Lopez-Sanchez, D. Lembke, M. Kayci, A. Radenovic and A. Kis, *Nat. Nanotechnol.*, 2013, **8**, 497–501.

S20 Z. Yin, H. Li, H. Li, L. Jiang, Y. Shi, Y. Sun, G. Lu, Q. Zhang, X. Chen and H. Zhang, *ACS Nano*, 2012, **6**, 74–80.

S21 D.-S. Tsai, K.-K. Liu, D.-H. Lien, M.-L. Tsai, C.-F. Kang, C.-A. Lin, L.-J. Li and J.-H. He, *ACS Nano*, 2013, **7**, 3905–3911.

S22 S. A. Svatek, E. Antolin, D.-Y. Lin, R. Frisenda, C. Reuter, A. J. Molina-Mendoza, M. Muñoz, N. Agraït, T.-S. Ko, D. P. de Lara and A. Castellanos-Gomez, *J. Mater. Chem. C*, 2017, **5**, 854–861.

S23 Y. Yang, N. Huo and J. Li, *J. Mater. Chem. C*, 2017, **5**, 7051–7056.